The 9th European Congress on Computational Methods in Applied Sciences and Engineering
ECCOMAS Congress 2024
3–7 June 2024, Lisboa, Portugal

MULTISCALE FINITE ELEMENT STUDY OF THE EFFECTS OF THE WATER RETENTION CURVE HYSTERESIS ON CHLORIDE INGRESS IN RECYCLED AGGREGATES CONCRETE.

Arthur FANARA*[1], Luc COURARD[2] and Frédéric COLLIN[3]

[1] Faculty of Applied Sciences, University of Liège, Belgium, arthur.fanara@uliege.be
[2] Faculty of Applied Sciences, University of Liège, Belgium, luc.courard@uliege.be
[3] Faculty of Applied Sciences, University of Liège, Belgium, f.collin@uliege.be

Key words: Finite Element Method, FE2, Fluid Mechanics, Multiscale, Multiphysics, Durability, Corrosion, Recycled Aggregates, Waste Management, Hysteresis

Summary. The use of Recycled Concrete Aggregates (RCA) in concrete provides a sustainable approach to limit the amount of Construction and Demolition Waste (CDW) that is landfilled, while preserving natural resources of aggregates. Recycled Aggregates Concrete (RAC)'s main challenge is its durability compared to Natural Aggregates Concrete (NAC). A significant risk to reinforced concrete structures is chloride infiltration, particularly in coastal or road environments.
A multiscale chemo-hydraulic model has been created using the Finite Element Squared (FE^2) method and has been verified and calibrated. The constitutive equations utilise intrinsic parameters derived from the experimental characteristics of concrete built in a laboratory. The model can replicate experiments with accuracy and provides a deeper insight into chloride ingress in both saturated and unsaturated concrete.
The hysteresis phenomena present in the water retention curve of granular materials is studied experimentally and implemented numerically according to the Van Genuchten formulation. The impact on chloride ingress is analysed, where the degree of saturation is a crucial factor in the transport mechanism.

1 INTRODUCTION

Durability is a key design element of the construction industry. Reinforced concrete structures are often expected to reach a service life superior to a century. Multiple degradation processes may reduce that expectancy, such as freeze-thaw cycles, carbonation, chloride attacks, or, in most cases, a combination of those [28, 24]. Many degradation processes require water as a transportation vector or as a reactant [25], as it is the case for chloride attacks. In a porous system such as concrete, the water and chloride ions transfer mechanisms are complex and depend on various intrinsic properties of the material. Characterising these transfers is therefore crucial to the understanding of durability in reinforced concrete subjected to chloride attacks. A dual approach is best in this case: the intrinsic properties of the materials are determined experimentally and used in a developed multiscale multiphysics model.

Water transfer properties are often dependent on the relative humidity of the environment and on the water saturation degree of the porous system. The latter is itself dependent on the composition of the material, among other. Concrete is made of a mixture of water, cement, sand and aggregates. The aggregates account for around 75% of the overall volume: they greatly influence the transfer properties of concrete, and must comply to several chemical, geometrical and physical properties [30]. Aggregates can be sourced naturally, industrially or through recycling of Construction and Demolition Wastes (CDW). In a world where cities are forced to renew their constructed park instead of continually expanding their boundaries, the demolition of old buildings is generating a huge stream of CDW, which contain concrete wastes for the most part. Recycled Concrete Aggregates (RCA) are sourced from crushing old concrete members during demolition, and contain a conglomerate of mortar and natural aggregates. Their properties are therefore dependent on the properties of the parent concrete (mainly its mechanical properties) as well as on the crushing process (type of crusher and number of crushing steps, mainly) [6, 29]. Standards are starting to introduce RCA into their pool of usable materials for concrete [4, 26], with specifications related to concrete made from recycled aggregates [5, 26] as well as for structural design [26].
Concrete made from RCA, referenced as Recycled Aggregates Concrete (RAC) in this research, have been investigated for decades. A lot of literature is based on their mechanical properties [14, 23] while few focused on their durability properties [21, 7]. In this paper, the durability is characterised through the concentration in chloride ions of the material. Chloride ions penetrate the porous system through diffusion in the pore solution or convection with water flows. They then concentrate near the steel rebars and eventually corrode them, once their concentration has reached a specific level. Many chloride ion critical concentration level have been found in the literature [31, 32], but this threshold is highly dependent on the oxygen level at the surface of the steel, which is itself related to the saturation degree of concrete [3]. If the threshold is defined as the level of chloride ions required to initiate the depassivation of the steel, then it can be taken equal to 0.4% by mass of cement [17, 31].

The chloride ingress is therefore highly dependent on the water content and flows, and the corrosion rate itself is also dependent on the saturation degree, with a maximum around 85% [1]. To characterise the behaviour of the porous structure of concrete with respect to water, several experiments have been performed [10, 11]: the porosity, water absorption, intrinsic water permeability and water retention curves of several materials have been determined. The latter expresses the evolution of the saturation degree inside the material porous matrix with respect to the environmental conditions, such as the relative humidity and temperature, through the expression of the matrix suction. Depending on the evolution trend of the environmental conditions, that is either sorption or desorption, the water retention curve is not identical [2]. Two phenomenon can explain this hysteresis: the ink-bottle effect, where water re-entering narrow pores require a local increase in suction, and the raindrop effect, due to the difference in contact angle between an advancing and a receding interface [2]. Depending on the history of the material, an infinity of path can be defined, in between the two main scanning curves. The history of the material is therefore important to know in order to determine its water transfer properties as well as its saturation degree.
Due to theses non-linearity, a multiscale multiphysics model has been developed to account for water flows in an unsaturated porous concrete, as well as for the diffusion and advection of

chloride ions inside the pore solution. The hysteresis of the water retention curve has been introduced and the characterisation of its influence on the chloride ingress is the scope of this paper.
First, the materials and methods are presented, with a focus on the experiment of static sorption and desorption, which yields the water retention curves of our materials. Then, the numerical double scale model is introduced and its constitutive equations are presented, along the modelling of the microstructure. Finally, the influence of the hysteresis on chloride ingress is studied.

2 Materials and Methods

Three materials have been characterised in this work:

1. NAC, a natural aggregate concrete with limestone 2/7 aggregates;
2. RAC, a recycled aggregate concrete with 2/7 RCA, with the same particle size distribution than the natural aggregates and with the same aggregate volume fraction than the NAC;
3. E-M, a mortar developed with the Concrete Equivalent Method [33, 9].

The composition of each material is presented in Table 1 for reproducibility purposes.

The goal of this experimental plan is to obtain properties for water and chloride transfer of our materials. The substitution of aggregate will be our focus, hence all our compositions have the same cement quantity and effective water-to-cement ratio.
The experimental plan is similar to that of Fanara et al. (2022) [10] and Fanara et al. (2023) [11], hence it will not be explained in details here. However, the method and results of the static sorption and desorption experiment are examined below.

Table 1: Composition and fresh properties of the materials characterised: NAC, RAC and E-M.

Composition	m_{agg} (kg/m^3)	m_{sand}	m_{cement}	m_{water}	W/C	Efficient W/C
NAC	1111	643	320	172.5	0.54	0.5
RAC	946	643	320	201.2	0.63	0.5
E-M	-	1337	622.5	336	0.54	0.54

2.1 Static Sorption and Desorption

The static sorption and desorption experiment aims to determine the main scanning curves of the water retention curves, for our three materials. The theoretical basis of that experiment is the vapour control method, based on the hypothesis that a hygroscopic material absorbs or releases water vapour depending on its saturation degree, until it reaches an equilibrium with the humid air it is in contact with. The equilibrium is achieved when the vapour pressure and temperature of both the porous medium and the ambient medium are equal [20].
A constant relative humidity is therefore defined through the use of a saline solution, the type and concentration of that solution dictating the value of the relative humidity, in combination with temperature that is kept constant. The samples are then enclosed in a sealed chamber with

the saline solution inside until they reach equilibrium [27, 8]. The Kelvin's law ties the suction to the relative humidity and temperature inside the chamber [10]:

$$s = \frac{\rho_w \, R \, T}{M} \ln(RH) \tag{1}$$

where s is the suction [MPa]. The ambient parameters are the relative humidity [-] (RH) and the temperature [K] (T), and R is the constant of perfect gases (equal to 8.3143 J/K.mol), M refers to the molar mass of water (equal to $18.016E{-}3$ kg/mol) and, finally, ρ_w is the density of water [kg/m^3].

The saline solutions used are shown in Table 2, along with their target RH and corresponding suction at 21°C. The real temperature and relative humidity is verified once a week while the total duration of the experiment is approximately three months, after which the sample is often in hygrometric equilibrium with the ambient air.

Table 2: Saline solution and their respective target RH [%] and suction [MPa] used for the determination of the water retention curves of our materials.

Saline Solution	KCl	NaCl	$Ca(NO_3)_2$	$MgCl_2$	Silica salt
Target RH [%]	90	75	56	35	6
Target Suction [MPa]	14.3	39.1	78.7	142.5	381

Once the sample water content is in equilibrium with its environment, the sample is weighed and, with its saturated and dry mass, its saturation degree can be determined. The water retention curve is then drawn to express the evolution of the saturation degree with suction. An empirical model is then used to draw that retention curve based on the five experimental points obtained, that is the Van Genuchten model [34]:

$$S_e = S_{res} + (S_{sat} - S_{res}) \left(1 + \left(\frac{s}{\alpha}\right)^n\right)^{-m} \quad \text{with} \quad m = 1 - \frac{1}{n} \tag{2}$$

where n is an adimensional model parameter related to the rate of desaturation of the soil and m is another adimensional model parameter related to the curvature (slope) of the water retention curve. The last model parameter, denoted α [Pa], is related to the air-entry pressure [10]. Finally, one can see the maximum saturation S_{sat} and the residual saturation S_{res}, as well as the suction s.
This empirical relationship is initially asymptotic in nature and is therefore only used to represent the water retention curve between the air-entry value and the residual value of the porous material [15]. Here the terms S_{res} and S_{sat} come into play to allow the modelling of the entire curve.

The hysteresis between both main scanning curves can be defined through a model based on the one of Van Genuchten. In this work, the model of Zhou et al. (2012) [36] is implemented. The main scanning curves of the water retention curves, defined by Equation 2, can be written

specifically for the drying curve (with a suffix d) and for the wetting curve (with the suffix w):

$$S_{ed} = S_{res} + (S_{max} - S_{res}) \left[1 + \left(\frac{s}{\alpha_d}\right)^{n_d}\right]^{-m_d} \tag{3}$$

$$S_{ew} = S_{res} + (S_{max} - S_{res}) \left[1 + \left(\frac{s}{\alpha_w}\right)^{n_w}\right]^{-m_w} \tag{4}$$

The hysteresis is then defined by the scanning curves (suffix s) [36]:

$$\frac{\partial S_{es}}{\partial s}(\text{drying}) = \left(\frac{s_d}{s}\right)^{-b} \left(\frac{\partial S_{ed}}{\partial s}\right) \text{ with } s_d = \alpha_d \left(S_e^{-1/m_d}\right)^{1/n_d} \tag{5}$$

$$\frac{\partial S_{es}}{\partial s}(\text{wetting}) = \left(\frac{s_w}{s}\right)^{b} \left(\frac{\partial S_{ew}}{\partial s}\right) \text{ with } s_w = \alpha_w \left(S_e^{-1/m_w}\right)^{1/n_w} \tag{6}$$

where the parameter b [-] is defined as a fitting parameter, always positive. It influences the gradient of the scanning curve, the closer it gets to zero and the more parallel the hysteresis curve is to the main curve, while the greater it is and the more horizontal the hysteresis curve gets [36].

The final saturation degree may then be obtained thanks to the derivative defined above and the increment in suction (ds) applied:

$$S_e^t = S_e^{t-1} + \left(\frac{\partial S_{es}}{\partial s}\right) \times ds \tag{7}$$

For accuracy purposes, the increment in suction ds has been limited to the value of the air-entry pressure, after a sensitivity analysis [12].

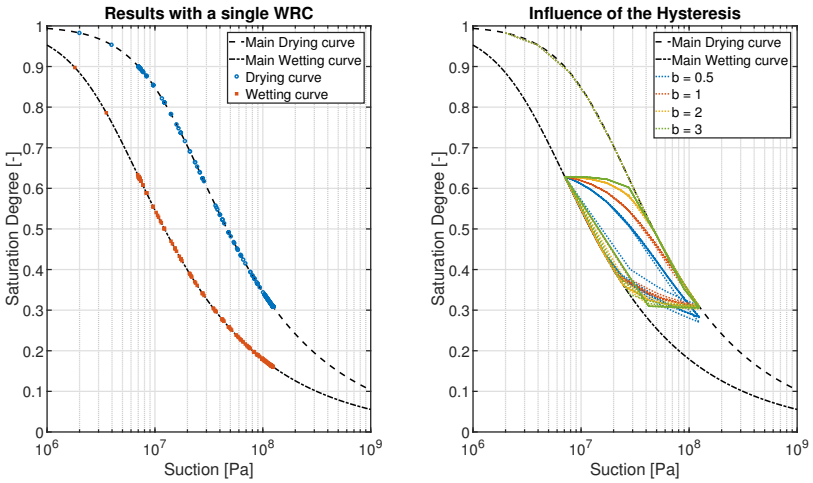

Figure 1: Example of main water retention curves along with hysteresis curves for several values of parameter b.

Of course, the two main scanning curves act as limits for the hysteresis curves: they define boundaries that may never be crossed. The saturation degree therefore depends on the history

of the material.

An example of main wetting and drying water retention curves, along with hysteresis curves for several values of b, is shown in Figure 1.

2.2 Experimental Results

The key results of the experimental campaign, as defined in Fanara et al. (2023) [11], are presented in Table 3. Most of these parameters are directly used in the numerical model implemented, hence their presence in this paper.

Table 3: Results of the experimental campaign

Parameter	**E-M**	**NAC**	**RAC**
Water absorption experiment			
Dry Density [kg/m^3]	2025	2263	2061
Porosity [% Volume]	22.83	14.16	20.5
Water permeability experiment			
Intrinsic Permeability [10^{-19}m^2]	38.7	1.73	2.58
Static sorption and desorption experiment			
n_{vG} (Desorption) [-]	1.35	1.39	1.36
n_{vG} (Sorption) [-]	1.4	1.38	1.36
α_{vG} (Desorption) [MPa]	6.23	8.16	7.2
α_{vG} (Sorption) [MPa]	0.77	0.41	0.54
Hysteresis b_1 [-]	0.8	0.85	0.75
Hysteresis b_2 [-]	1.1	1.2	1.2
Diffusion under unsteady-state			
D_{app} [10^{-11}m^2/s at 15/29/91 days]	1.71/1.43/0.92	1.77/1.41/2.77	2.46/1.65/1.78

3 FE^2 Model

The numerical model is developed following a FE^2 scheme, which consists of four iterative steps carried out at every macroscale's Gaussian point:

1. The boundary conditions of the macroscale are localised into gradients and mean values, which serve as boundary conditions at the subscale;
2. The boundary value problem at the subscale is solved by finite element analysis;
3. Homogenisation of the subscale fluxes to obtain a unique value per macroscale integration point;
4. The macroscale boundary value problem is solved by finite element analysis.

Three degrees of freedom are implemented: water and gas pressures, and chloride ions concentration. This allows to consider either saturated or unsaturated conditions. The constitutive equations used to govern those degrees of freedom are Darcy's law and Fick's law for the advection of water and gas, and the diffusion of chlorides, respectively. The subscale and macroscale constitutive equations may be found in details in Fanara et al. (2024) [12].

3.1 Representative Volume Element

In a FE² model, the subscale is represented by a Representative Volume Element (RVE), whose aim is to incorporate the specific material heterogeneities one wants to implement in the model. In this work, the relevant heterogeneities are caused by the replacement of aggregates: the RVE is a section of concrete, several centimetres in size, made up of impermeable natural aggregates surrounded by adherent mortar (in the case of recycled concrete aggregates), which are then incorporated into a homogenised mortar paste with its own homogenised properties [35]. Figure 2 shows two RVEs representing both Natural Aggregate Concrete (NAC) and Recycled Aggregate Concrete (RAC).

Each phase of the RVE, namely the adherent mortar or new mortar matrices (the aggregates are impervious and therefore not represented numerically), has unique intrinsic homogenised properties used in subscale constitutive equations. There is one exception: the water retention curve, which is intrinsically homogenised at the macroscale. Some authors could argue that the Interfacial Transition Zone (ITZ) is required in the definition of the RVE [22, 19]. However, our model is based on experimental intrinsic properties, and characterising the ITZ is not yet possible in a precise manner. It was therefore excluded from this model.

Two methods of generating a RVE are particularly suitable for building materials: image analysis and algorithm development [18]. The latter is prefered in this work as it allows to modify the RVE based on mix properties rather than requiring the acquisition of a new image at each modification of the mix, which is necessary for the former. However, it is less precise than RVE based on image analysis. For this work, an algorithm was developed, which requires several intrinsic properties of the material mixture:

- Particle Size Distribution (PSD) of the aggregates only;
- Surface Fraction (SF) of the aggregates within the mixture, which in this study is equal to their volumetric fraction;
- Aspect Ratio (AR) of the aggregates.

The algorithm is explained in Fanara et al. (2022) [13]. Once the RVE is generated, it is meshed using the gmsh software from the University of Liège [16].

4 Study of the Influence of the Hysteresis

One parameter is of crucial importance while implementing the hysteresis model: the fitting parameter b, controlling the gradient of the scanning curve [36]. It is obtained through fitting of the experimental sorption and desorption experiments, that are rather laborious and extensive. Furthermore, depending on the history of the material, the value of b may not be unique.
In this section, the impact of the value of this parameter b on the results of our hysteresis model is studied. The intrinsic properties of our materials, that is NAC and RAC, used in the model, are listed in Table 3, with the value of the chloride diffusion coefficient set at 29 days. Because the mesh of the mesoscale only represents the permeable mortar, the implemented mesoscale properties (porosity, intrinsic permeability, and chloride diffusion coefficient) are those of the E-M composition, multiplied by 1.3 to account for the difference between a 2D and 3D model

[12]. The water retention curve, however, is a macroscale property: the parameters implemented correspond to either NAC or RAC, depending on the mesoscale used.

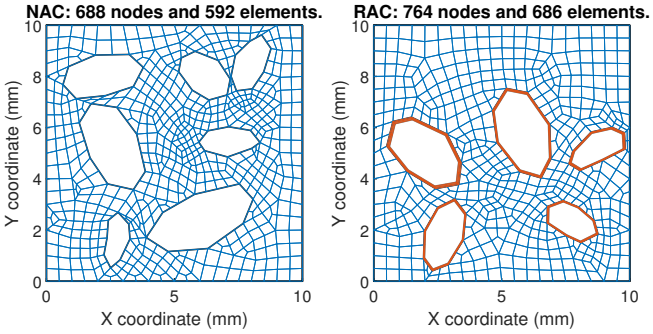

Figure 2: RVE representing the mesoscale of both NAC (left) and RAC (right), with properties of the E-M composition for the blue mortar phase (new mortar matrix) and the same properties for the orange mortar phase (adherent mortar of the RCA).

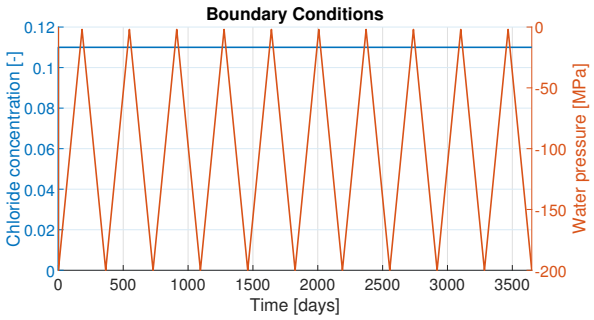

Figure 3: Boundary conditions for the study of the influence of the parameter b on the hysteresis model.

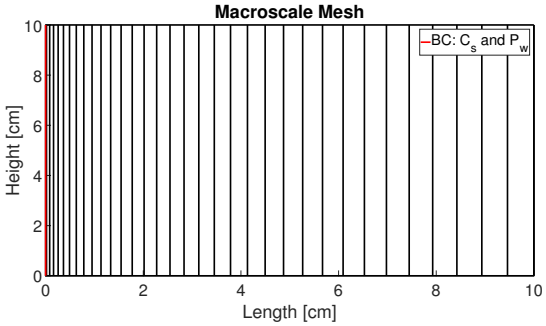

Figure 4: Macroscale mesh for the study of the influence of both the increment of suction and the parameter b on the hysteresis model.

The mesoscales of NAC and RAC are shown in Figure 2. The macroscale, on the other hand, represents a 1D sample that is 10cm long and is displayed in Figure 4. For this simulation, the initial water pressure conditions inside the sample were equal to the atmospheric pressure. The pressure on the outside border varies bi-annually from -2MPa to -200MPa, and back, for a period of ten years. Furthermore, the outside border is set to have a chloride content of 0.11 [-], while the inside of the sample is initially free of chloride. The boundary conditions are shown in Figure 3.

Figure 5 displays the water retention curves of the NAC and RAC, for various values of b. Two simulations were conducted without the hysteresis of the water retention curve, using properties of the boundary drying or wetting curves. It is seen that the higher the value of b, the faster the hysteresis reaches the boundary curves, the scanning curve being more horizontal. Additionally, the saturation degree throughout the NAC has a greater variation range than the RAC.

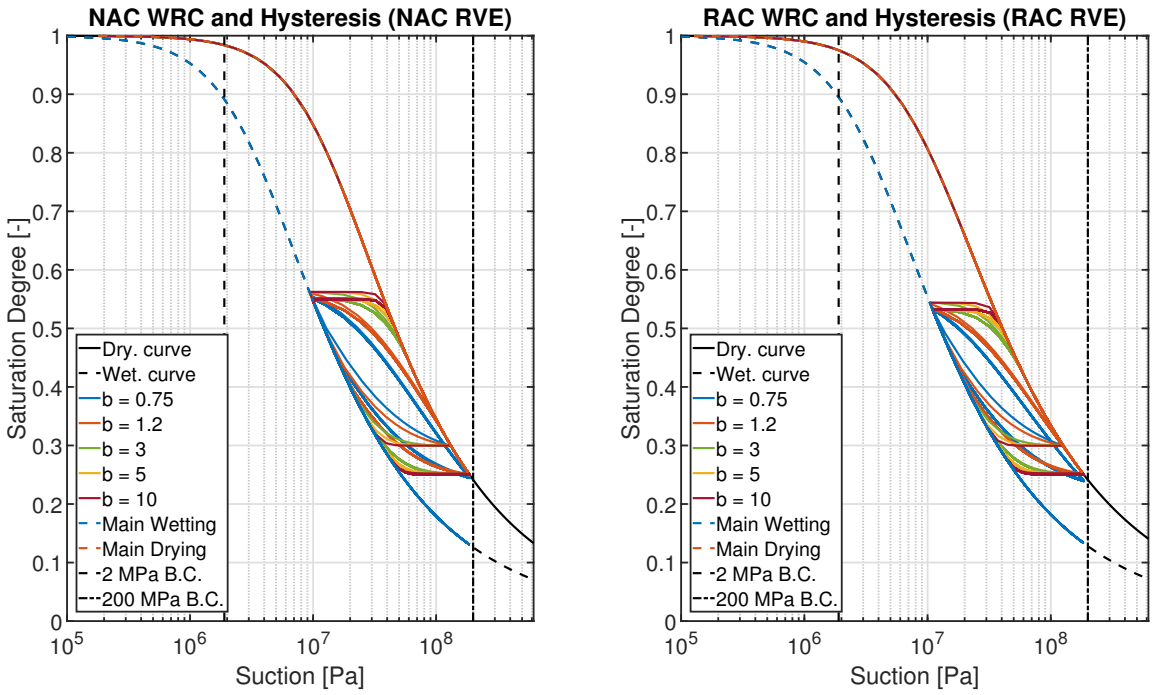

Figure 5: Influence of the parameter b on the hysteresis model: Water Retention Curves for the NAC and RAC.

Figure 6 shows the chloride content evolution at depths of 0cm, 2cm, 5cm, and 10cm (from the top to the bottom of the Figure, respectively) for both NAC and RAC, over a ten-year period.
As the value of b increases, the variations between drying and wetting phases decrease and the water saturation degree evolves more linearly. Consequently, the chloride content at greater depth is greater for the higher values of b. Furthermore, the boundary conditions have a smaller impact at greater depth, the diffusion being predominant over the advection of chloride ions and the effect of the bi-annual variations being smoothed. On the contrary, the difference between the values of b is negligible at the surface, due to the direct application of the boundary conditions.
Finally, the saturation degree and chloride content are positively correlated, as supported by simulations without the hysteresis: the sample with the boundary drying curve consistently exhibits higher chloride content than the one with the boundary wetting curve.

The conclusion of this sensitivity analysis on the value of the fitting parameter b is dual: firstly, the necessity to implement the hysteresis model has been proven, as the chloride content is greatly overestimated (or underestimated) if the model only uses the boundary drying (resp. wetting) curve. Additionally, the necessity to obtain and use the correct value of b has also been demonstrated, as it greatly influences the flow and the final content of chloride ions.

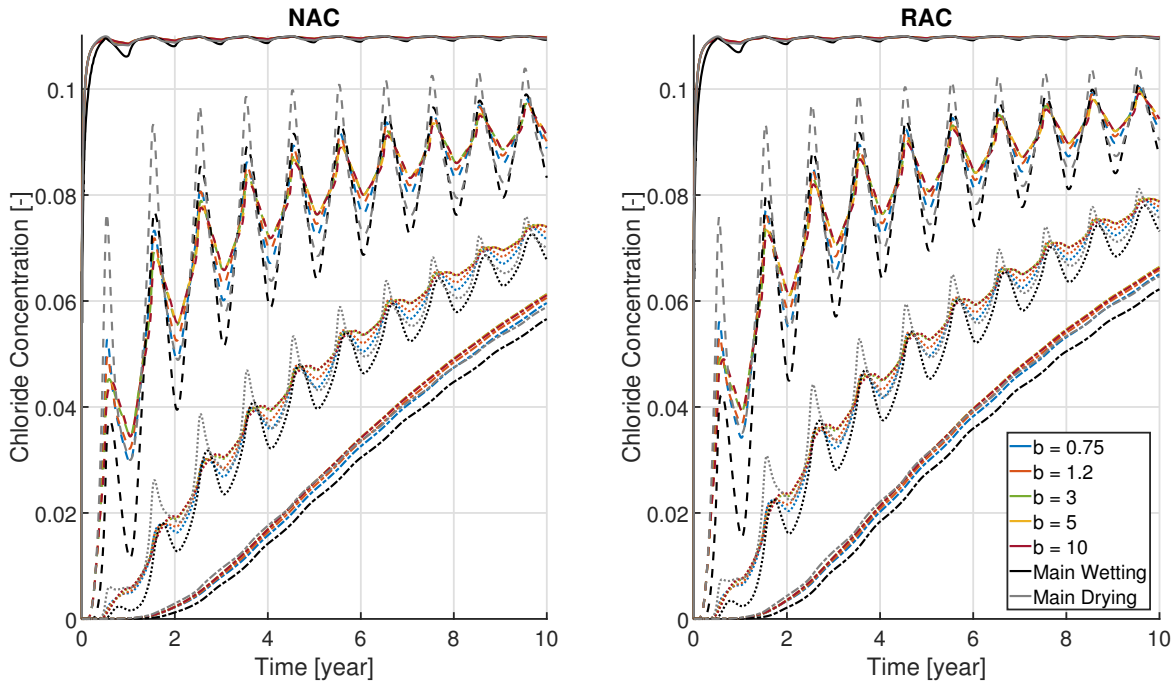

Figure 6: Influence of the parameter b on the hysteresis model: Chloride Content of NAC (left) and RAC (right) at 0, 2, 5 and 10cm depth (from top to bottom) over a ten-year period.

5 Conclusion

This paper studies the implementation of a hysteresis model for the water retention curves of concrete. Water retention curves are a necessary tool for modelling unsaturated conditions in porous materials. However, the hysteresis phenomenon associated to those curves is often neglected numerically. For the development of this multiscale model, the Van Genuchten model (1980) [34] was implemented for the boundary drying and wetting curves, along with the hysteresis model by Zhou et al. (2012) [36] that is compatible with the one of Van Genuchten.
Experiments were conducted on concretes made of natural aggregates and recycled concrete aggregates, as well as on a mortar. It yielded numerous parameters necessary for the implemented constitutive equations. The hysteresis model was experimentally calibrated to accurately replicate unsaturated conditions of concrete made from natural or recycled aggregates.
The developed multiscale model was used for a sensitivity analysis on the value of b, the fitting parameter for the hysteresis model. To better understand the influence of b, the chloride ingress inside concrete was studied, as it is strongly dependent on the saturation degree of the porous system. Results have shown that higher values of b correspond to higher chloride content at higher depth.

When comparing the results of our study between the NAC and RAC, it was experimentally found that the RAC has a smaller (or higher) air-entry pressure for the boundary drying (or wetting) curve. This means that the exchange of moisture with the environment takes place sooner than for the NAC. The parameter n_{vG}, which corresponds to the rate of (de)saturation, is

rather similar for both compositions. If we consider the chloride content of the two compositions, the chloride content of the RAC tends to be higher than that of the NAC, which is logical because of the greater movement of water between the sample and its environment, and the greater chloride diffusion coefficient of the RAC.

Acknowledgements

Funding: This work is supported by the Wallonia regional government (Belgium) in the framework of a FRIA (Fund for Industrial and Agricultural Research) grant.

REFERENCES

[1] I. Balafas and C. J. Burgoyne. Environmental effects on cover cracking due to corrosion. *Cement and Concrete Research*, 40:1429–1440, 2010.

[2] J. Bear and A. Verruijt. *Modeling Groundwater Flow and Pollution*. D. Reidel Publishing Company, 1987.

[3] L. Bertolini, B. Elsener, P. Pedeferri, and R. P. Polder. *Corrosion of Steel in Concrete*. WILEY-VCH Verlag GmbH and Co. KGaA, Weinheim, 2004.

[4] CEN. EN-12620+A1 - Aggregates for concrete, with 2008 amendment. Technical report, Brussels, Belgium, 2008.

[5] CEN. EN-206 - Concrete: Specification, performance, production and conformity. Incorporating corrigendum May 2014. Technical report, Brussels, Belgium, 2013.

[6] M. S. de Juan and P. A. Gutiérrez. Study on the influence of attached mortar content on the properties of recycled concrete aggregate. *Construction and Building Materials*, 23:872–877, 2009.

[7] F. Debieb, L. Courard, S. Kenai, and R. Degeimbre. Mechanical and durability properties of concrete using contaminated recycled aggregates. *Cement & Concrete Composites*, 32:421–426, 2010.

[8] P. Delage, M. Howat, and Y. Cui. The relationship between suction and swelling properties in a heavily compacted unsaturated clay. *Engineering Geology*, 50:31–48, 1998.

[9] T. K. Erdem, K. H. Khayat, and A. Yahia. Correlating Rheology of Self-Consolidating Concrete to Corresponding Concrete-Equivalent Mortar. *ACI Materials Journal*, 106(2):154–160, March-April 2009.

[10] A. Fanara, L. Courard, and F. Collin. Development of a fe^2 multiscale model of chloride ions transport in recycled aggregates concrete. 2022.

[11] A. Fanara, L. Courard, and F. Collin. Numerical and experimental study of chloride ion transport in recycled aggregates concrete. *Academic Journal of Civil Engineering*, 40(2):Vol 40 No 2 (2022): Special Issue–NoMaD 2022, 2023.

[12] A. Fanara, L. Courard, and F. Collin. Numerical FE^2 Study of Chloride Ingress in Unsaturated Recycled Aggregates Concrete. *Available at SSRN: https://ssrn.com/abstract=4756062*, 2024.

[13] A. Fanara, L. Courard, F. Collin, and J. Hubert. Transfer properties in recycled aggregates concrete: Experimental and numerical approaches. *Construction and Building Materials*, 326:126778, 2022.

[14] G. Fathifazl, A. G. Razaqpur, O. B. Isgor, A. Abbas, B. Fournier, and S. Foo. Creep and drying shrinkage characteristics of concrete produced with coarse recycled concrete aggregate. *Cement and Concrete Composites*, 33:1026–1037, 2011.

[15] D. G. Fredlund, D. Sheng, and J. Zhao. Estimation of soil suction from the soil-water characteristic curve. *Canadian Geotechnical Journal*, 48:186–198, 2011.

[16] C. Geuzaine and J.-F. Remacle. Gmsh: A 3-d finite element mesh generator with built-in pre- and post-processing facilities. *International Journal for Numerical Methods in Engineering*, 79(11):1309–1331, May 2009.

[17] O. E. Gjørv. Durability of Concrete Structures. *Arabian Journal for Science and Engineering*, 36:151–172, 2011.

[18] V. Holla, G. Vu, J. J. Timothy, F. Diewald, C. Gehlen, and G. Meschke. Computational Generation of Virtual Concrete Mesostructures. *Materials*, 14(14):3782, July 2021.

[19] Z. Hu, L. Mao, J. Xia, J. Liu, J. Gao, J. Yang, and Q. Liu. Five-phase modelling for effective diffusion coefficient of chlorides in recycled concrete. *Magazine of Concrete Research*, 70(11):583–594, 2018.

[20] S. J. Kowalski. *Thermomechanics of Drying Processes*. Springer-Verlag Berlin Heidelberg GmbH, 2003.

[21] S. M. Levy and P. Helene. Durability of recycled aggregates concrete: a safe way to sustainable development. *Cement and Concrete Research*, 34:1975–1980, 2004.

[22] Q. Liu, D. Easterbrook, J. Yand, and L. Li. A three-phase, multi-component ionic transport model for simulation of chloride penetration in concrete. *Engineering Structures*, 86:122–133, 2015.

[23] P. S. Lovato, E. Possan, D. C. C. D. Molin, Â. B. Masuero, and J. L. D. Ribeiro. Modeling of mechanical properties and durability of recycled aggregate concretes. *Construction and Building Materials*, 26:437–447, 2012.

[24] P. S. Mangat and B. T. Molloy. Prediction of long term chloride concentration in concrete. *Materials and Structures*, 27:338–346, 1994.

[25] M. Morga and G. C. Marano. Chloride Penetration in Circular Concrete Columns. *International Journal of Concrete Structures and Materials*, 9(2):173–183, Feb. 2015.

[26] J. N. Pacheco, J. de Brito, and M. L. Tornaghi. *Use of recycled aggregates in concrete: opportunities of upscaling in Europe*. JRC131294. Publications Office of the European Union, Luxembourg, 2023.

[27] M. Pap, A. Mahler, and S. G. Nehme. Analysis and Finite Element Modelling of Water Flow in Concrete. *Periodica Polytechnica Civil Engineering*, Oct. 2018.

[28] R. A. Patel, P. Janez, and J. Diederik. Multi-scale modeling strategies to improve durability models for service life predictions of concrete structures. In G. D. Schutter, N. D. Belie, A. Janssens, and N. V. D. Bossche, editors, *XIV DBMC - 14th International Conference on Durability of Building Materials and Components*, pages 309–310, Ghent University, Belgium, May 2017. RILEM.

[29] D. Pedro, J. de Brito, and L. Evangelista. Influence of the use of recycled concrete aggregates from different sources on structural concrete. *Construction and Building Materials*, 71:141–151, 2014.

[30] D. Pedro, J. de Brito, and L. Evangelista. Performance of concrete made with aggregates recycled from precasting industry waste: influence of the crushing process. *Materials and Structures*, 48(12):3965–3978, Nov. 2014.

[31] M. Raupach and T. Büttner. *Concrete Repair to EN 1504: Diagnosis, Design, Principles and Practice*. CRC Press, Taylor and Francis Group, 2014.

[32] A. V. Saetta, R. V. Scotta, and R. V. Vitaliani. Analysis of Chloride Diffusion into Partially Saturated Concrete. *ACI Materials Journal*, 90(5):441–454, 1993.

[33] A. Schwartzentruber and C. Catherine. La méthode du mortier de béton équivalent (MBE) - Un nouvel outil d'aide à la formulation des bétons adjuvantés. *Materials and Structures*, 33(8):475–482, Oct. 2000.

[34] M. T. Van Genuchten. A Closed-form Equation for Predicting the Hydraulic Conductivity of Unsaturated Soils. *Soil Science Society of America Journal*, 44:892:898, September 1980.

[35] Y. Xi and Z. P. Bažant. Modeling Chloride Penetration in Saturated Concrete. *Journal of Materials in Civil Engineering*, 11(1):58–65, Feb. 1999.

[36] A.-N. Zhou, D. Sheng, S. W. Sloan, and A. Gens. Interpretation of unsaturated soil behaviour in the stress – Saturation space, I: Volume change and water retention behaviour. *Computers and Geotechnics*, 43:178–187, June 2012.